



MIXED MODE FRACTURE OF BRICK

X. XIAO¹, N.G. SHRIVE²

Abstract

Mixed-mode fracture testing of brick, using three point bending has been conducted to obtain basic fracture data for masonry. Different notch depths and offset ratios were used. To understand cracking of masonry fully, it is essential to understand the fracture mechanisms of brick under mixed-mode loading. The crack initiation angles, final failure path, mixed-mode stress-intensity factor, energy release rate were investigated. Results indicate that there are two potential cracking paths when brick is subject to this mixed-mode loading: i.e., from the notch tip or the mid-span. The mixed-mode stress intensity factor K_C , energy release rate G_C and J-integral J_C decrease with increasing offset ratio.

Key Words

Masonry, Mixed-Mode Fracture, Three-Point Bending, Fracture Parameters.

1 Introduction

Crack propagation has been studied extensively. Much research has been concentrated on developing generalized fracture propagation theories involving mixed mode fracture (eg: Erdogan and Sih, 1963; Hussain et al, 1974; Sih, 1974) and developing techniques to calculate stress intensity factors (Chan et al., 1970; Park, 1974; Hellen, 1975; Ishikawa, 1980; Sha, 1984; Sha and Yang, 1990). Mixed-mode fracture in concrete has been a topic of several theoretical and experimental studies (eg: Arrea and Ingraffea, 1982, Rots et al., 1985, Wium et al., 1984, Kobayashi et al., 1985, and Ingraffea and Gerstle, 1985).

Here, a combined experimental and analytical investigation into mixed mode crack propagation in brick is described. The experimental program consisted of tests on series of three bricks with different notch depths and different offset ratios under three

¹ X.XIAO, PhD Student, Department of Civil Engineering, University of Calgary, Calgary, Alberta T2N 1N4, Canada. E-mail: xiao@ucalgary.ca.

² N.G. SHRIVE, Professor, Department of Civil Engineering, University of Calgary, Calgary, Alberta T2N 1N4, Canada. E-mail: shrive@ucalgary.ca

point bending. The FRANC2D (Cornell Fracture Group, 2003) code was used to analyse crack initiation and propagation, and calculate fracture parameters. The crack initiation angles, final failure path, mixed-mode stress-intensity factor (K) and energy release rate (G) were investigated. The ratio of K_{II}/K_I decreased as the Mode I stress intensity factor began to dominate. FRANC2D and the experiments allowed the determination of peak load, crack extensions, crack mouth opening displacements and final crack trajectories in varying mixed-mode stress fields at the tip of the growing cracks.

2 Material Test and Testing Specimens

Three solid clay bricks with different strengths were used in the tests: Granville Gray Titan Solid (A), Cinnamon Titan Solid (B) and Columbia Solid (C), all manufactured by I-XL Industries, Medicine Hat, Alberta. The dimensions of the bricks are 190mm x 90mm x 63mm (length x width x height). The material properties of the bricks, determined according to CAN3-A82.2-M78 (1978), are given in Table 1. Specimen details are listed in Table 2. The notches were formed with a masonry saw to provide a range of notch to depth ratios from 1/6 to 2/3. The notch to depth ratio is a/H as shown in Figure 2. The offset ratios are 25mm and 50mm from the centre line of the brick.

Table 1. Material Properties of three bricks

Brick type	Absorption (%)	Compressive strength (MPa)	Modulus of rupture (MPa)
A	8.0	60.6	5.3
B	7.7	93.0	7.2
C	10.3	72.8	6.7

Table 2 Specimen Details: 6 specimens of each type were tested; the combinations were repeated for bricks B and C

Specimen	Notch-to-depth Ratio (a_0/H)	Off-set ratio (mm)	Specimen	Notch-to-depth Ratio (a_0/H)	Off-set ratio (mm)
AOA	10.5	0	AMC	31.5	25
AOB	21	0	AMD	42	25
AOC	31.5	0	AEA	10.5	50
AOD	42	0	AEB	21	50
AMA	10.5	25	AEC	31.5	50
AMB	21	25	AED	42	50

Specimen naming rule: The first character stands for the brick; the second stands for the off-set ratio (O, M, E); the third stands for the notch depth (A for a notch-to-depth ratio of 1/6, B for 2/6, C for 3/6, D for 4/6).

3 Experimental Arrangement

The test arrangement is shown in Figures 1 and 2. The notched beams were tested in three-point bending in a closed-loop, electro-hydraulic MTS Test Machine at a crosshead speed of 0.015mm/min. The complete crack mouth opening displacement (CMOD)-Load curve was obtained. When the off-set ratio was zero, the tests were pure mode I three-point bend tests. Material parameters (K_{IC} and CMODc) can be determined directly from the mode I test. When the off-set ratio was nonzero, a mixed-mode type of failure was expected to occur. The applied load, crack mouth opening displacement, and load-line displacement were monitored and stored with a digital oscilloscope. CMOD and load-line deflection were measured using MTS clip gauge and LVDT's, respectively.

Specimens with different off-set ratios were used to study the effect of Mode II shear. Specimens with the same off-set ratios but different notch-depth ratios were used to study the effect of notch depth on mixed-mode failure.

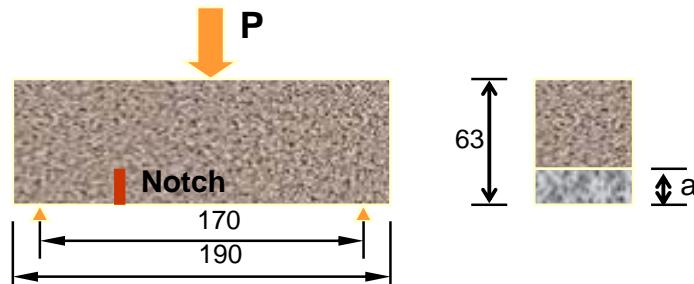


Fig.1 Test Configuration

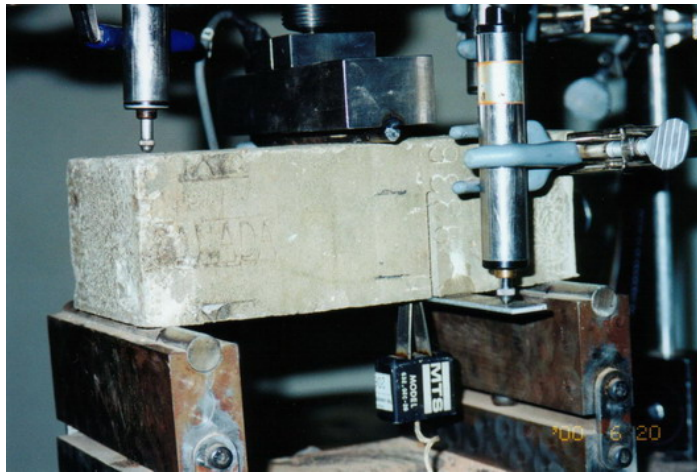


Fig.2 Mixed-mode test setup, showing clip gauge in brick and LVDT's at support and load line

4 EXPERIMENTAL RESULTS AND DISCUSSION

The maximum loads, final failure angles and other related information for Brick A are listed in Tables 3.

Table 3 Experimental Results for Solid Brick A

Specimen	Peak Load (KN)	Final Failure Angle(C ⁰)	Comment	Specimen	Peak Load (KN)	Final Failure Angle(C ⁰)	Comment
AOA-1	3.398	85		AMA-1	4.089	16	
AOA-2	3.642	90		AMA-2	3.904	15	
AOA-3	3.287	87		AMA-3	4.011	17	
AOA-4	3.564	90		AMA-4	3.441	14	
AOA-5	3.856	88		AMA-5	4.102	16	
AOA-6	3.365	90		AMA-6	3.637	15	
AOB-1	1.865	90		AMB-1	2.471	15	
AOB-2	2.315	85		AMB-2	2.566	18	
AOB-3	2.475	90		AMB-3	2.500	16	
AOB-4	1.986	88		AMB-4	2.648	13	
AOB-5	2.064	90		AMB-5	2.205	14	
AOB-6	2.212	90		AMB-6	2.498	12	
AOC-1	1.065	87		AMC-1	1.528	14	
AOC-2	1.437	88		AMC-2	1.581	16	
AOC-3	1.403	90		AMC-3	1.581	18	
AOC-4	1.324	90		AMC-4	1.625	19	
AOC-5	1.289	88		AMC-5	1.697	17	
AOC-6	1.265	90		AMC-6	1.644	20	
AOD-1	0.620	87		AMD-1	0.832	3	
AOD-2	0.542	90		AMD-2	0.817	13	
AOD-3	0.589	90		AMD-3	0.807	16	
AOD-4	0.498	90		AMD-4	0.861	18	
AOD-5	0.578	90		AMD-5	0.854	20	
AOD-6	0.496	84		AMD-6	0.851	15	
AEA-1	5.767	25		AEC-1	-	19	
AEA-2	5.499	-	Failure at centre	AEC-2	2.252	24	
AEA-3	5.665	22		AEC-3	2.419	22	
AEA-4	5.535	23		AEC-4	2.424	21	
AEA-5	5.747	21		AEC-5	2.321	32	
AEA-6	6.030	20		AEC-6	2.240	23	
AEB-1	3.320	21		AED-1	1.044	25	
AEB-2	3.322	29		AED-2	0.797	13	
AEB-3	3.117	27		AED-3	0.922	21	
AEB-4	3.553	25		AED-4	1.163	15	
AEB-5	3.463	23		AED-5	0.921	20	
AEB-6	3.295	23		AED-6	1.131	20	

4.1 Failure Mode and Cracking Path

The cracking trajectories of brick A are shown in Fig.3. In specimens with shallow notch depths, the cracking paths are more tortuous and associated with mixed mode behaviour. In specimens with deep notch depths, the cracking paths are more straight. The initial angle was assumed as the final failure angle. The tortuosity of cracking paths makes it difficult to measure the crack initiation angle, so the angle was measured from the notch tip to the final failure point.

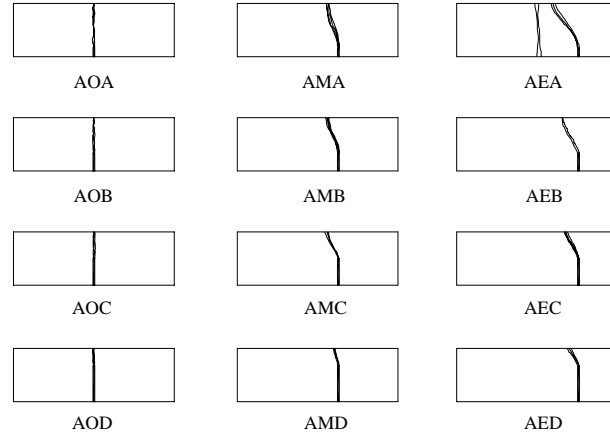


Fig. 3 Cracking Path of Specimens (Brick A, Granville Gray)

For the mixed-mode tests, there are two possible locations of failure, i.e., the notch tip and the mid-span (AEA in Fig.3). The failure at mid-span mostly occurred in specimens CEA and CEB. For other specimens, failure occurred from the notch tip.

The mixed-mode stress intensity factor (K_C) was defined as

$$K_C^2 = K_I^2 + K_{II}^2 \quad (1)$$

Based upon the principle of Linear Elastic Fracture Mechanics, the energy release rate G_C can be expressed in terms of the stress intensity factors as (Broek, 1982):

$$G = \frac{K_I^2}{E'} + \frac{K_{II}^2}{E'} \quad (2)$$

Where

$E' = E$ for plan stress

$E' = E/(1-\nu^2)$ for plane strain

E = Young's modulus

ν = Poisson's ratio

K_I = mode I stress intensity factor

K_{II} = mode II stress intensity factor

Methods of predicting mixed crack propagation aim to: (1) determine the direction of crack initiation and extension; and (2) determine the load at which the extension will occur according to some criterion. At present, analytic models can be classified as those which are based purely in fracture mechanics and those which depend on other (classical) failure theories. The most commonly used mixed-mode fracture criterion is the fracture mechanics parabolic relationship:

$$\left(\frac{K_I}{K_{IC}} \right)^2 + \left(\frac{K_{II}}{K_{IIC}} \right)^2 \geq 1 \quad (3)$$

We used FRANC2D to analyse crack initiation and propagation, and calculate fracture parameters. A Young's modulus of 20GPa and Poisson's ratio of 0.19 were used for the brick. FRANC2D uses eight-noded quadrilateral elements with quadratic shape functions. The crack tip is modelled using a rosette of six-noded triangular elements. Cracking paths are shown in Fig. 4 using FRANC. Results for the fracture parameters are presented in Table 4. For the sake of brevity, only experimental results of brick A are reported here.

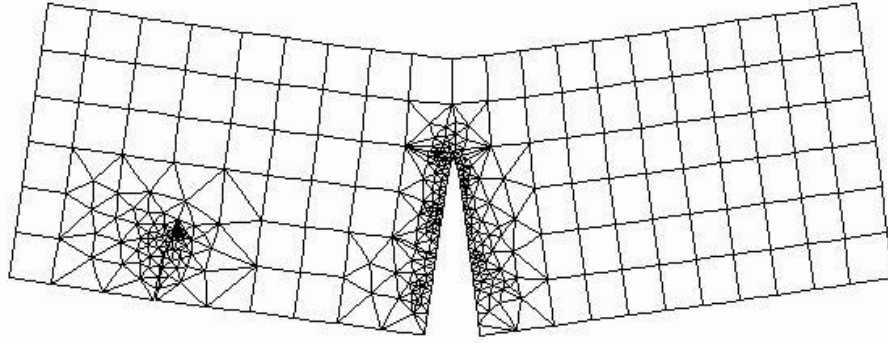


Fig. 4 Cracking Paths of Brick under Mixed-Mode Condition

Table 4 Fracture Parameters of Brick

Specimen	K_C ($\text{kNm}^{-3/2}$)	G_C (Nm^{-1})	J_C (Nm^{-1})
AOA	418	781	794
AOB	401	736	746
AOC	375	655	670
AOD	303	429	469
AMA	382	650	662
AMB	384	672	684
AMC	382	682	699
AMD	346	566	613
AEA	339	515	524
AEB	307	431	438
AEC	309	499	509
AED	228	248	261

4.2 Typical Load-CMOD Curve

Crack mouth opening displacement (CMOD) is the amount the crack opens at the base of the specimen. The CMOD was measured with a standard clip gauge (MTS Model 632.02). A typical load versus CMOD curve (ascending and descending branch) obtained from the experiments is shown in Fig.5. Non-linearity is observed near the peak load. The Load-CMOD curve is linear to about 80% of the peak load, followed by non-linear behaviour. The nonlinear behaviour can be due to microcracking and slow crack growth.

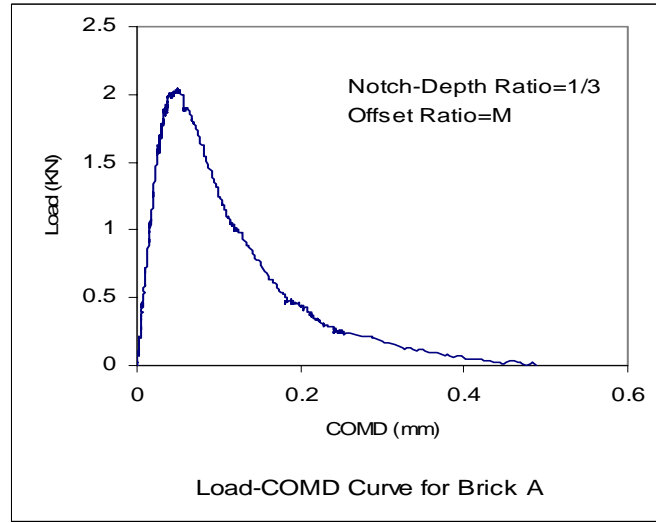


Fig.5 Typical Load-CMOD Curve

4.3 Peak Load vs Offset Ratio and Notch-Depth Ratio

The experimental results of the peak loads versus offset ratios are shown in Fig.6. There exists a critical offset ratio γ_c , when $\gamma < \gamma_c$, the failure always occurs at the notch tip, and when $\gamma > \gamma_c$, the failure occurs at the mid-span. When $\gamma = \gamma_c$, the failure could occur at either the notch tip or the mid-span. γ_c is different for the different bricks. γ_c is termed the transition stage (John and Shah, 1988). At the transition stage, the measured peak load corresponding to failure at the notch tip seems like that corresponding to failure at the mid-span.

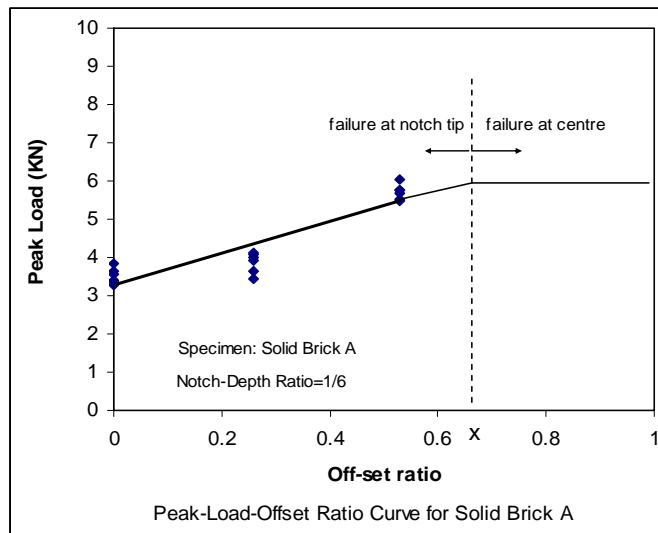


Fig.6 Peak Load-Offset Ratio Curve for Brick A

John and Shah (1988) investigated mode I and mixed-mode fracture of concrete subjected to impact and static loading. They reported that for the values of γ_c between 0.7 and 0.77. Failure occurred at the notch under impact loading, whereas under quasi-static loading the failure occurred at mid-span. γ_c is shown arbitrarily at 0.67 in Fig.6.

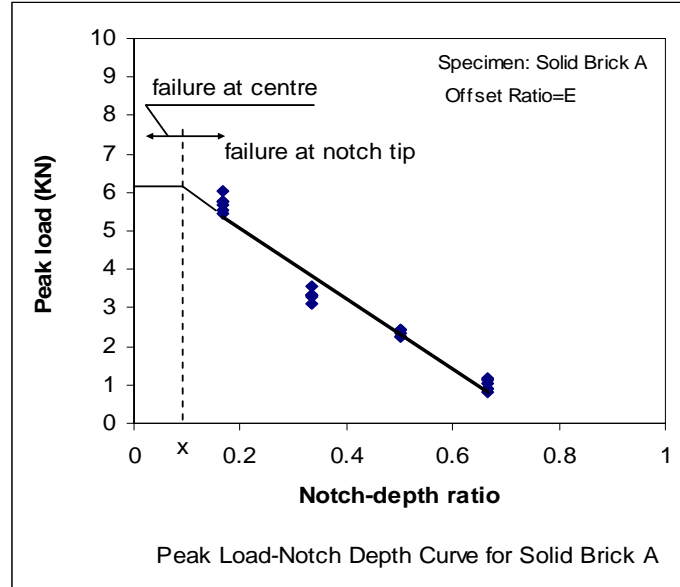


Fig.7 Peak Load-Notch Depth Curve for Brick A

The experimental results of the peak loads versus notch depths are shown in Fig.7. Like γ_c , there exists a critical notch-depth ratio α_c . When $\alpha > \alpha_c$, failure initiates at the notch tip, and when $\alpha < \alpha_c$, the failure occurs at the mid-span. When $\alpha = \alpha_c$, the crack could propagate from either the notch tip or the mid-span. α_c is shown arbitrarily at 0.1 in Fig.7.

It is difficult to determine α_c and γ_c experimentally, requiring extensive tests for different types and strength of brick.

4.4 Fracture Parameters

The stress intensity (K_C), energy release rate (G_C) and J-integral for brick A are listed in Table 4. The stress intensity factor decreases (K_C) with offset ratio, as shown in Fig. 8. The variations of G_C and J_C with offset ratio are very similar. The stress intensity factors K_C in Table 4 are of the same order of magnitude, but slightly lower than those of concrete (Ratanalert S. and Wecharatana M., 1989).

Analysis indicates K_{II}/K_I increases with increasing offset ratio, In contrast to Swartz et al (1988, 1998) concerning mixed mode fracture of concrete, the mixed mode stress intensity K_C here is not greater than the Mode I stress intensity K_{IC} because of the

absence of aggregate. K_{II}/K_I ratios of the specimens tested are relatively small, so the assumption of a traction-free crack is probably valid.

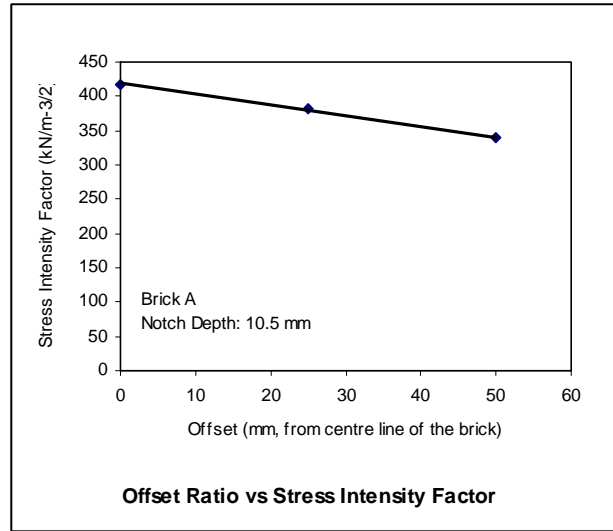


Fig.8 Stress Intensity Factor Decreases with Increscent Offset Ratio

5 Conclusions

1. The Crack initiation angle is about 15 to 25 degrees, depending on the location of the notch in the specimen. The crack path is not smooth but tortuous and is associated with mixed mode behaviour due to friction.
2. There are two possible cracking paths when a brick is under the mixed-mode loading used here: i.e., from the notch tip or mid-span. There exists a critical offset ratio γ_c , when $\gamma < \gamma_c$, failure always occurs at the notch tip, and when $\gamma > \gamma_c$, failure initiates from mid-span. When $\gamma = \gamma_c$, the failure could occur at either the notch tip or the mid-span.
3. The mixed-mode stress intensity factor K_C , energy release rate G_C and J-integral J_C decrease with increasing offset ratio.
4. In contrast to mixed mode fracture of concrete, the mixed mode stress intensity is not greater than the Mode I stress intensity because of absence of aggregate.
5. K_{II}/K_I increases with increasing offset ratio.

Acknowledgment

We gratefully acknowledge the support of the National Sciences and Engineering Research Council of Canada (NSERC) and I-XL Industry, Medicine Hat, Alberta, Canada.

References

- Arrea M., Ingraffea A. R., 1982, Mixed-mode Crack Propagation in Mortar and Concrete, Master thesis, Department of Structural Engineering, Cornell University: Ithaca, New York.
- Broek D., 1982, Elementary Engineering Fracture Mechanics, Martinus Nijhoff Publishers, the Netherlands.
- Canadian Standard Association, 1978, CAN3-A82.2-M78, Methods of Sampling and Testing Brick, Rexdale, Ontario
- Chan S.K., Tuba I.S., Wilson, W.K., 1970, On the finite element method in linear fracture mechanics, Engineering Fracture Mechanics 2, 1-s17.
- Cornell Fracture Group, 2003, FRANC2D V.31, Cornell University.
- Erdogan F., Sih, S.C., 1963, On the crack extension in plates under plane loading and transverse shear, Journal of Basic Engineering ASME 85, 5 19-525.
- Hellen T.K., 1975, On the method of virtual crack extensions. International Journal for Numerical Methods in Engineering 9, 87-207.
- Hussain M.A., Pu S.L., Underwood, J., 1974, Strain energy release rate for a crack under combined model and mode II. Fracture Analysis, ASTM STP 560, 2-28.
- Ingraffea A.R., Gerstle W.H., 1985, Application of Fracture Mechanics to Cementitious Composites. S.P. Shah, ed., Kluwer Academic Publishers, Dordrecht, the Netherlands
- Ishikawa H. 1980, A finite element analysis of stress intensity factors of combined tensile and shear loading by only a virtual crack extension. International Journal of Fracture 16, 243-246.
- John R., Shah S.P., 1988, Mixed-mode fracture of concrete subjected to impact loading, Journal of Structural Engineering, 116 (3), 585-602.
- Kobayashi A. S., et al., 1985, Application of Fracture Mechanics to Cementitious Composites. S.P. Shah, ed., Kluwer Academic Publishers, Dordrecht, the Netherlands
- Parks D.M. 1974, A stiffness derivative finite element technique for determination of crack tip stress intensity factors. International Journal of Fracture 10, 487-502.
- Rots J.G., et al, 1985, HERON 30, 1.
- Ratanalert S. and Wecharatana M., 1989, Evaluation of Existing Fracture Models in Concrete, Fracture Mechanics: Application to Concrete, Victor C. Li and Zdenek P. Bazant, eds, ACI, SP-118.
- Sha G.T. 1984, On the virtual work extension technique for stress intensity factors and energy release rate calculations for mixed fracture mode, International Journal of Fracture 25, 33-42.
- Sha, G.T., Yang, C.T. 1990, Use of analytically decoupled near tip displacement solutions for calculating the decoupled weight functions of mixed fracture modes. Engineering Fracture Mechanics 37, 59 1-610.
- Sih G.C. 1974, Strain-energy-density factor applied to mixed crack problems. International Journal of Fracture 10, 305-321.
- Swartz S.E., Lu L.W., Tang L.D., 1988, Mixed-mode fracture toughness testing of concrete beams in three-point bending, Materials and Structures 21, 33-40.
- Swartz S.E., Lu L.W., Tang L.D., Refai T.M.E., 1998, Mode II fracture –parameter estimates for concrete from beam specimens, Experimental Mechanics 28, 146-153
- Wium D. J. W., Buyukozturk O., L.V. C., 1984, Hybrid Model for Discrete Cracks in Concrete. Journal of Engineering Mechanics, ASCE, 110(8), 1211-1229.